Science of the Total Environment 797 (2021) 149056

Contents lists available at ScienceDirect

Science of the Total Environment

journal homepage: www.elsevier.com/locate/scitotenv

Coastal riverine wetland biogeochemistry follows soil organic matter distribution along a marsh-to-mangrove gradient (Florida, USA)

Sarah A. Harttung [a], Kara R. Radabaugh [b], Ryan P. Moyer [b], Joseph M. Smoak [c], Lisa G. Chambers [a,*]

[a] Department of Biology, University of Central Florida, 4000 Central Florida Blvd, Orlando, FL 32816, United States of America
[b] Florida Fish and Wildlife Conservation Commission, Fish and Wildlife Research Institute, 100 8th Ave SE, St. Petersburg, FL 33701, United States of America
[c] School of Geosciences, University of South Florida, 140 7th Ave S, St. Petersburg, FL 33701, United States of America

HIGHLIGHTS

- Three Florida Gulf coast riverine marsh-mangrove ecotones were studied.
- Vegetation ecotones were not a proxy for biogeochemical ecotones.
- Soil biogeochemical patterns differed from river to river across the landscape.
- Organic matter was the most informative metric of soil biogeochemical patterns.
- Inorganic nutrient concentrations were strongly seasonal.

GRAPHICAL ABSTRACT

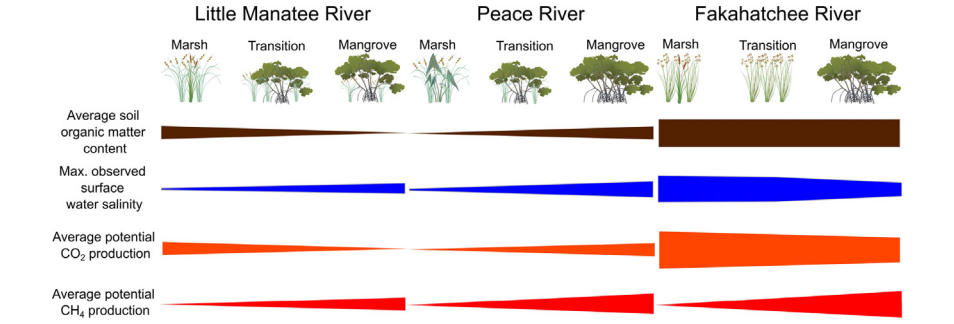

ARTICLE INFO

Article history:
Received 29 April 2021
Received in revised form 28 June 2021
Accepted 12 July 2021
Available online 16 July 2021

Editor: Ouyang Wei

Keywords:
Habitat switching
Sea-level rise
Greenhouse gases

ABSTRACT

Many subtropical coastal wetland vegetation communities are transitioning from herbaceous marsh to woody mangrove, often facilitated by sea-level rise. This study investigated the relationships between vegetation community (upstream marsh, ecotone/transition, and downstream mangrove), salinity (S), and soil biogeochemistry in wetlands along three rivers on the Florida Gulf coast (the Little Manatee, Peace, and Fakahatchee Rivers). Vegetation was surveyed, and soil and water samples were collected during both the dry and the wet season and analyzed for biogeochemical properties (soil: bulk density, pH, organic matter, extractable inorganic and total nutrients, dissolved organic carbon (DOC), and microbial biomass carbon; water: inorganic nutrients and DOC) and processes (greenhouse gas production) while salinity and water level were continuously monitored in the field. Results indicated landscape-scale patterns in soil biogeochemistry differed significantly by river and were most strongly correlated with soil organic matter content, regardless of vegetation community or salinity regime. Contrary to expectations, soil organic matter content gradients were not always inversely related to salinity gradients, and methane production was observed in moderate- ($S = 12$) and high- ($S = 34$) salinity mangrove communities. The vegetation ecotone experienced seasonally variable salinity and did not serve as a true biogeochemical intermediate between the marsh and mangrove communities. This study demonstrates the need for site-specific studies of biogeochemical gradients in coastal wetlands and indicates the marsh-to-mangrove ecotone is not a proxy for salinity or biogeochemical tipping points. Instead, soil organic matter content is suggested as the most relevant indicator of biogeochemical properties and processes in wetlands along coastal rivers, superseding vegetation community or salinity.

* Corresponding author.
E-mail address: lisa.chambers@ucf.edu (L.G. Chambers).

https://doi.org/10.1016/j.scitotenv.2021.149056
0048-9697/

1. Introduction

Coastal wetland ecosystems range from salt marshes in temperate climates to mangrove forests in the tropics and provide a host of ecosystem services, including storm surge buffering, nutrient removal, water storage, wildlife habitat, and carbon storage (Barbier et al., 2011; Costanza et al., 1998; Sun et al., 2018). In the subtropics, many marshes are transitioning into mangrove-dominated ecosystems (Coldren et al., 2019; Eslami-Andargoli et al., 2009; Giri and Long, 2016; Kelleway et al., 2016; Liu et al., 2017). While the frequency of intense freeze-events dictates latitudinal mangrove expansions (Cavanaugh et al., 2014), sea-level rise and decreased freshwater flow are important drivers of landward mangrove transgression in areas where the areal extent is not limited by temperature (Krauss et al., 2011). An increase in salinity can give mangroves a competitive advantage over less salt-tolerant brackish and freshwater marsh vegetation (Spalding and Hester, 2007), and, as long as propagules are present, mangroves can fill the void left by dead and dying glycophytes (Herbert et al., 2015). This shift from herbaceous to woody vegetation changes both aboveground ecophysiology and belowground biogeochemistry. For example, mangroves are taller and store more carbon aboveground than marshes (Kelleway et al., 2016), and young mangroves in Florida can cycle nutrients more rapidly than neighboring salt marsh (Steinmuller et al., 2020). Roots of *Avicennia germinans* in a mesohaline system can grow nearly half a meter into the soil (Purvaja et al., 2004), possibly stimulating local microbial activity in previously anoxic wetlands (Ball, 1988).

As mangroves gradually transgress landward within coastal wetland landscapes, their encroachment co-occurs with the existing gradients of topography, salinity, and tidal inundation. Generally, soil organic matter (OM) content and nutrient concentrations (carbon (C), nitrogen (N), and phosphorous (P)) are highest near the freshwater end of the coastal salinity gradient, decreasing downstream to the saltwater end-member community (Craft, 2007; Loomis and Craft, 2010; Morrissey et al., 2014; Odum, 1988; Twilley and Chen, 1999; Wieski et al., 2010; Williams et al., 2014). Salinity alone can alter biogeochemical processes in these nutrient-rich freshwater tidal wetlands, which in turn, affects the rates in which carbon dioxide (CO_2) and methane (CH_4) are emitted from soil as end-products of microbial mineralization. Vegetation can become stressed by the heightened salinity and therefore reduce root growth (Conner et al., 1997; Wilson et al., 2018), which further alters substrate availability for microbial respiration and could lead to a decline in CO_2 production (Neubauer et al., 2013). In other wetland soils, saltwater intrusion increases soil respiration and nutrient flux into the water column. For example, laboratory incubations of freshwater soils with low ($S = 0.5$), moderate ($S = 14$), and high ($S = 35$) salinity seawater increased CO_2 production for two weeks after the onset of saline conditions (Chambers et al., 2011). In a flow-through reactor, freshwater soils exposed to artificial seawater ($S = 10$) released bound PO_4^{3-} and NH_4^+ (Weston et al., 2006). However, this stimulation effect may be short-term, as overall CO_2 flux decreased by 83% in surface soils (0–3 cm) after 3.5 years when porewater salinity increased from 0.5 to 2–5 (Neubauer et al., 2013).

Saltwater intrusion can also shift dominant pathways of microbial respiration in soils as the abundant sulfate in saline wetlands allows sulfate-reducing prokaryotes to outcompete methanogens in highly reduced soils (Capone and Kiene, 1988). Methanogenesis usually decreases dramatically when freshwater soils are introduced to low-salinity water (Chambers et al., 2011, 2013; Edmonds et al., 2009; Helton et al., 2014; Livesley and Andrusiak, 2012; Neubauer, 2013; Weston et al., 2006). Salinity as low as one has been found to suppress methanogenesis in favor of sulfate reduction in the Cape Fear estuary in North Carolina, USA (Hackney and Avery, 2015), while $S = 10$ was identified as the threshold between CH_4 and CO_2 dominance in tidal freshwater marsh soils in China (Wang et al., 2017). However, others have demonstrated methane production can be sustained into low and moderate salinity ranges (Bartlett et al., 1987; Wang et al., 2017; Weston et al., 2011) and sometimes reaches a local maximum at oligo- or mesohaline wetlands (Weston et al., 2014; Poffenbarger et al., 2011).

Due to the co-occurrence of mangrove encroachment and the salinity gradients known to influence biogeochemistry, we sought to investigate the utility of highly visible shifts in vegetation communities in serving as a proxy for local saltwater intrusion and accompanying changes in biogeochemical properties and processes. For example, does the landward extent of mangroves reflect a tipping point in the salinity regime, and can anything be deduced about C, N, and P cycling patterns simply based on observed vegetation transitions? Specifically, the objectives of this study were to 1) investigate physicochemical gradients and soil biogeochemical properties and processes along three coastal riverine wetland vegetation gradients from marsh to mangrove communities and 2) determine if the biogeochemical gradients observed across the ecotone are consistent across the landscape (i.e., among the three study rivers). In other words, are readily observable vegetation communities a robust indicator of other physical, chemical, and biological properties in coastal wetlands? An observational field study was conducted in the coastal wetlands along three subtropical tidal rivers on Florida's Gulf coast using a three-site transect that spanned the marsh-mangrove ecotone to meet these objectives. Soil and water samples were collected in both the dry and the wet seasons to account for the effects of changing abiotic conditions. We expected the upstream marsh would have the highest concentrations of nutrients, soil OM, and CH_4 production, all of which would progressively decrease as one moves downstream into the transition and mangrove communities. We further expected spatial patterns in biogeochemical properties from marsh to mangrove would remain consistent across the landscape, regardless of river, and be primarily driven by salinity, as reflected by the dominant vegetation community.

2. Methods

2.1. River descriptions

This study was conducted along the west coast of central and south Florida, each characterized by a humid subtropical or tropical climate. The region has a dry season from November to April and a wet season from May to October. Study transects were established on the Little Manatee River (near Ruskin, FL), the Peace River (near Arcadia, FL), and the Fakahatchee River (south of Naples, FL). Three sampling locations (referred to as sites) were established along each river based on the dominant vegetation community: marsh (upstream), transition (midway with mixed vegetation), and mangrove (downstream) (Fig. 1). Site location, establishment and sampling dates, and soil series information for all rivers are in Supplementary Table 1. Fakahatchee River, in the southwest portion of the Greater Everglades, was uniquely characterized by a large, sheet-flow-dominated wetland mosaic with few shallow channels, rather than the comparatively deep and well-defined channels seen at the Little Manatee and Peace Rivers. These attributes limited access and the ability to choose sites along a defined river transect in the Fakahatchee basin. Therefore, marsh, transition, and mangrove sites were chosen based on observable differences in the dominant vegetation community within the mosaic (Fig. 1). Vegetation cover and biomass were assessed in 10×10 m plots between July and October 2018, using a modification of methods outlined in Radabaugh et al. (2018) to confirm that each site accurately represented the desired vegetation community. HOBO data loggers (models U24-002-C and U20-04; OnSet Computer Corporation, Bourne, MA, USA) housed in a single 1.2-m-long, 6-cm-wide PVC piezometer with 0.2-mm-wide slits along the length (22 slits per 10 cm) monitored conductivity and water level every 30 min. Piezometers were installed at each site within the intertidal zone by hammering the PVC into the soil until resistance.

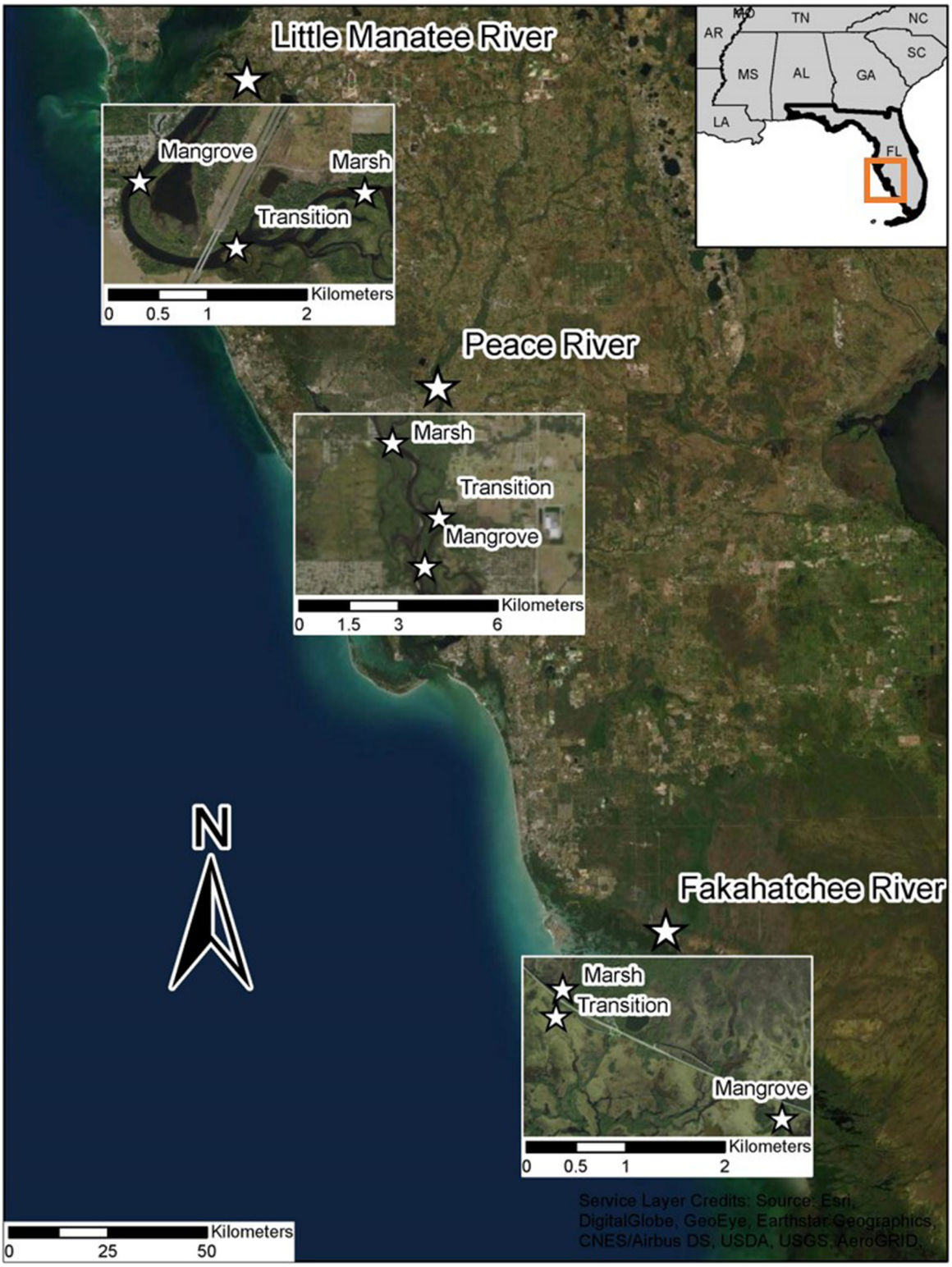

Fig. 1. Map of sampling locations across the west coast of Florida, USA.

Loggers were pushed to the bottom of the piezometers to ensure submergence for as much of the study period as possible. Sites were sampled during both the dry and the wet seasons (March–April and October 2018), at which point logger data were also downloaded and malfunctioning equipment identified and replaced. Salinity is reported in practical salinity units (psu), which is a unitless measurement of salinity and practically interchangeable with parts per thousand (ppt) (Reid, 2011).

2.2. Sampling design

During each sampling event, three soil cores extending to a depth of 30 cm were taken in the intertidal zone at each site within 1 m in the upstream (dry season sampling) or downstream (wet season sampling) direction of the piezometer using the push core method. Specific sampling locations within this area were chosen haphazardly to avoid coring directly on live stems. Core tubes were made of 7-cm-diameter

polycarbonate with a beveled edge. A rubber mallet and wooden board were used to pound the tube into the soil with limited soil compaction. Each core was extruded and sectioned in the field into four segments: 0–5 cm, 5–10 cm, 10–20 cm, and 20–30 cm. The 5-cm increment at the top of the core was chosen to account for what has been shown to be the most biologically active layer in wetland soils (Koretsky et al., 2005; Kostka et al., 2002) All analyses described below were performed on all depth segments. Samples were stored in polyethylene bags on ice for transport to the laboratory and kept at 4 °C until analysis. Surface water samples were also collected at each site during soil collection. Surface water samples were filtered through 0.45-μm Whatman® 42 filters (Cytiva Life Sciences, Marlborough, MA, USA) upon return to the lab, acidified with one drop of double-distilled (DD) H_2SO_4, and stored at 4 °C until nutrient and dissolved organic carbon (DOC) analysis within 28 days. Surface water nutrients NO_x^-, NH_4^+, and PO_4^{3-} were quantified on a SEAL AQ2 Automated Discrete Analyzer (Seal Analytical, Mequon, WI). Published detection limits for these methods were 0.003 mg L^{-1}, 0.002 mg L^{-1}, and 0.004 mg L^{-1} for NO_x^-, NH_4^+, and PO_4^{3-}, respectively. Detailed analytical procedures for all laboratory methods are available in Supplementary Table 3. The surface water salinity was determined in the field using a YSI ProDSS (YSI/Xylem Inc., Yellow Springs, OH, USA), and all values are reported on the practical salinity scale (Lewis, 1980).

2.3. Soil and water properties

A subsample of homogenized soil for each depth segment was dried at 70 °C in a gravity oven for three days, or until sample weight stabilized, to obtain dry bulk density (DBD) and moisture content. Any rhizomes were removed before drying, but other root material was retained. Dried soil was ground with ceramic balls in a SPEX 8000 M Mixer/Mill (SPEX Sample Prep, Metuchen, NJ, USA) for 2 min. The proportion of soil OM was calculated as the proportion of weight lost by a dried ground subsample following ashing in a muffle furnace at 550 °C for 3 h (Craft et al., 1991). Total P was measured on the ashed sample following the method developed by Andersen (1976). Briefly, 50 mL of 1 N HCl were added to ashed samples, which were then heated to boiling for 30 min on a hot plate. Once cooled to room temperature, samples were filtered through 0.45-μm Whatman® 42 filters (Cytiva Life Sciences, Marlborough, MA, USA) and diluted to 50 mL to account for evaporative volume loss. Total P was determined colorimetrically (EPA-134-A Rev. 5; US EPA 1993) on a SEAL AQ2 Automated Discrete Analyzer (SEAL Analytical, Mequon, WI). Total C and total N were quantified by folding 5 μg of dried, ground soil into a tin capsule and combusting using an Elementar vario MICRO select (Elementar Analytical, Langenselbold, Germany. A 1:5 soil: deionized water slurry was mixed and allowed to equilibrate for 1 h as described by Thomas, 1996 (with modifications) for pH to be measured on an Accumet XL200 benchtop pH probe (Thermo Fisher Scientific, Waltham, MA, USA).

2.4. Extractable inorganic nutrients and dissolved organic C

Extractable inorganic nutrients NO_x^- (EPA-126-A Rev. 9), NH_4^+ (EPA-129-A Rev. 8;), and PO_4^{3-} (EPA-145-A Rev. 1; US EPA 1993) from non-fumigated samples from microbial biomass C analysis were analyzed colorimetrically on a SEAL AQ2 Automated Discrete Analyzer (Seal Analytical, Mequon, WI). Published detection limits for these methods were 0.01, 0.05, and 0.005 mg L^{-1}, for NO_x^-, NH_4^+, and PO_4^{3-}, respectively. Shimadzu TOC-L Analyzer (Shimadzu Scientific Instruments, Kyoto, Japan) results from non-fumigated samples were used to determine extractable DOC concentrations. The published detection limit for this method is 50 μg TC L^{-1}.

2.5. Microbial biomass C

Microbial biomass C was measured with the chloroform fumigation method described in Vance et al. (1987) with modifications (Steinmuller et al., 2020). Duplicate soil samples of 5 g were weighed together upon return to the laboratory: one to be fumigated and one as a non-fumigated control. Non-fumigated samples were extracted with 25 mL 2 M KCl and incubated in an orbital shaker for 1 h at 25 °C and 150 rpm, centrifuged for 10 min at 5000 rpm and filtered through 0.45-μm Whatman® 42 filters (Cytiva Life Sciences, Marlborough, MA, USA) at the time the duplicate samples were fumigated. Once extracted, samples were acidified with one drop of DD H_2SO_4. After chloroform fumigation for 24 h in a vacuum desiccator, samples were extracted using the same process as the non-fumigates. Fumigates and non-fumigates were analyzed on a Shimadzu TOC-L Analyzer (Shimadzu Scientific Instruments, Kyoto, Japan) using the non-purgeable organic C base method (detailed analytical procedures are available in Supplementary Table 2). Microbial biomass C (mg kg^{-1}) was calculated as the difference in concentration between fumigated and non-fumigated samples.

2.6. Potential soil CO_2 and CH_4 production

Soil (10 g) from each depth of the core sections were added to a 120 mL serum vial upon return to the laboratory. Any coarse roots were removed from the soil, but the fine roots remained. Vials were crimped-capped with a rubber septum and stored at 4 °C overnight. The following day, vials were evacuated for 1-minute using a vacuum. After evacuation, vials were purged with N_2 gas for 3 min to ensure an anaerobic environment. Then, 16 mL of anaerobic site water filtered through a 0.45-μm Whatman® 42 filter (Cytiva Life Sciences, Marlborough, MA, USA) was added to create the slurry from which potential rates of soil CO_2 and CH_4 production were determined. Site water was made anaerobic before mixing with soil by purging the filtered water with N_2 gas for 20 min. Soil slurries were incubated in an orbital shaker at 25 °C and 150 rpm. Headspace samples were taken with a glass gas-tight syringe every 24 h for five days and immediately analyzed on a Shimadzu GC-2014 equipped with a flame ionized detector (FID) and methanizer (Shimadzu Scientific Instruments, Kyoto, Japan) to determine CO_2 and CH_4 concentrations. Gas production rates were calculated as either CO_2 or CH_4 concentration over time, employing soil pH and Henry's Law to account for gas in the dissolved phase. The effects of pressure and temperature on gas solubility were calculated with the ideal gas law (Weiss, 1974; See Supplementaty Material for details and equations).

2.7. Data analysis

All sites are referred to as marsh, transition, or mangrove, depending on the dominant vegetation community. Statistical analyses were performed using R version 3.4.1 (RCoreTeam, 2019) within the RStudio "Orange Blossom" 1.2.5033 environment (RStudioTeam, 2020). Data were assessed for normality and homogeneity of variance using the Shapiro-Wilks test and Levene's test, respectively, and visually via histograms. The R package fitdistplus (Delignette-Muller and Dutang, 2015) was used to determine each parameter's best distribution, as almost all parameters, except for pH and moisture content, were non-normally distributed. If two distributions were identified as the best fit, both models were run. The model with the lowest AICc score was chosen. Generalized linear models with a Gaussian or gamma distribution with identity and log links were often used to assist with interpretation. Model structure varied depending on the parameter, which can be seen in Table 2. At first, all parameters were run through an ANCOVA with the following structure: parameter ~ Organic matter proportion (covariate) + River * Site + Season + Depth. After running this first complex model, simplified models were run and passed through AICc to determine which terms best fit the model. Type III error was specified in the ANCOVA summaries to reduce the chance of rejecting the null hypothesis for the wrong reason at $\alpha = 0.05$.

3. Results

3.1. River characteristics

3.1.1. Little Manatee River

Moving downstream from the marsh to the mangrove site, species diversity and herbaceous biomass decreased while canopy cover and woody biomass increased. The vegetation community at the marsh site was dominated by *Juncus roemerianus, Typha* sp., and *Acrostichum danaeifolium*, the transition site by *J. roemerianus, Typha* sp., and *A. danaeifolium* with *Rhizophora mangle* seedlings and a single mature *R. mangle*, and the mangrove site by *R. mangle*. Average canopy cover at the sites increased from 14.3% at the marsh site (no woody aboveground biomass) to 27.9% at the mangrove site (4.42 Mg ha^{-1} aboveground woody biomass). Total aboveground biomass was lowest at the marsh site and highest at the transition and mangrove sites (10.2, 25.1, and 21.4 Mg ha^{-1}, respectively; Fig. 2).

Water level deviations were similar among the three sampling sites (Fig. 3A). Generally, the average tidal range increased from the transition (0.36 ± 0.19 m) to the mangrove site (0.44 ± 0.08 m). Surface water salinity measured during the seasonal soil samplings indicated an increase of nearly 6 salinity units between the upstream (marsh) and downstream (mangrove) sites during the dry season (Supplementary Table 2). In contrast, wet season salinity at all sites was less than 1. Weekly salinity was variable during the dry season and early wet season (March–June) at the mangrove site, ranging from 12 in March to 2 at the beginning of June (Fig. 3D). Concentrations of surface water NO_x^- were below detection in the dry season and increased to approximately 0.2 mg L^{-1} in the wet season. Concentrations of NH_4^+ in surface water followed the opposite pattern, decreasing by about 88% in the wet season compared to the dry season. Surface water PO_4^{3-} concentrations roughly doubled from the dry to the wet season. Generally, surface water DOC concentrations showed no seasonal trends (Supplementary Table 2).

3.1.2. Peace River

The marsh was the only site on the Peace River's main channel, while the transition and the mangrove sites were both located on Hunters Creek, a braided sub-channel of the main river (Fig. 1). The marsh site was dominated by mixed herbaceous species and *A. danaeifolium,* the transition site by *Shoenoplectus tabernaemontani*, *Typha* sp., and *A. danaeifolium* with a few *R. mangle* seedlings, and the mangrove site by *R. mangle* and *A. danaeifolium*. Average canopy cover increased moving downstream, from 7.8% at the marsh site to 85.2% at the mangrove site. Woody biomass and canopy cover increased moving downstream. Aboveground total biomass and woody biomass were lowest at the marsh (16.3 and 1.5 Mg ha^{-1}, respectively) relative to the transition (23.1 and 9.5 Mg ha^{-1}, respectively) and mangrove sites (156.5 Mg ha^{-1}; Fig. 2).

Sites displayed similar patterns in water level, tidal range, and salinity fluctuations. Water levels fluctuated seasonally (Fig. 3B). Tidal ranges were also similar (0.39 ± 0.1 m at the mangrove site to 0.45 ± 0.1 m at the transition site). Discrete surface-water salinity measurements indicated a ~ 5-unit increase from the marsh to the mangrove site during the dry season (all sites within the oligo- to mesohaline range), while all sites were fresh (S < 0.5) during the wet season (Supplementary Table 2). Dry season salinity was dynamic at all sites, for example, varying up to 15 within a single week (S = 3–18) at the mangrove site (Fig. 3E).

Across all sites, surface water concentrations of NO_x^- were 61, 10.8, or 5.7 times higher in the wet season than the dry season for the marsh, transition, and mangrove sites, respectively. Dry season NO_x^- concentrations displayed a slight low-to-high gradient from the marsh to the mangrove site. Season had little effect on both NH_4^+ and PO_4^{3-} concentrations. Dry season PO_4^{3-} concentrations decreased slightly from the marsh site to the mangrove site. In the wet season, surface water DOC concentrations were 25–35% lower at the marsh and mangrove sites. The transition site saw a 114% increase in surface water DOC in the wet season (Supplementary Table 2).

3.1.3. Fakahatchee River

Notably, the marsh site was located north of a major highway (US 41, or Tamiami Trail) known to restrict water flow through the Greater Everglades (Krauss et al., 2018). The transition and mangrove sites were located south of US 41. *Typha* sp. dominated the river channel at the marsh site, *Muhlenbergia capillaris* dominated the transition site, and the mangrove site was in a stand of *Laguncularia racemosa.* Neither the marsh site nor the transition site had woody biomass, nor did the mangrove site have herbaceous biomass. Total aboveground biomass was lowest at the marsh and transition sites (42.7 and 44.2 Mg ha^{-1}, respectively) and highest at the mangrove site (Fig. 2). The average canopy cover at the mangrove site was 89.3%, and aboveground woody biomass was 131.8 Mg ha^{-1}.

All three sites experienced a significant dry-down during the 2018 dry season, dipping far below the mean continuous water level recorded during the sampling period (Fig. 3C). At the end of the wet season, water levels at the marsh and the mangrove sites began to fall while rising at the transition site. Average daily ranges in water column depth were small, from 5 ± 8 cm at the marsh and transition to 7 ± 8 cm at the mangrove site and appeared to be driven by evapotranspiration. Of the three sites, the marsh site displayed the greatest difference in salinity between samplings, while the mangrove site had the greatest range in water level fluctuation. Discrete sampling indicated high salinity during the dry season, equivalent to full-strength seawater in the marsh and the transition sites. The mangrove site was brackish, possibly because of a closer hydrologic connection to a constructed ditch along US 41 (Fig. 1; Supplementary Table 2). Continuous salinity data revealed hypersaline conditions (S = ~ 45) at the marsh site in late May 2018.

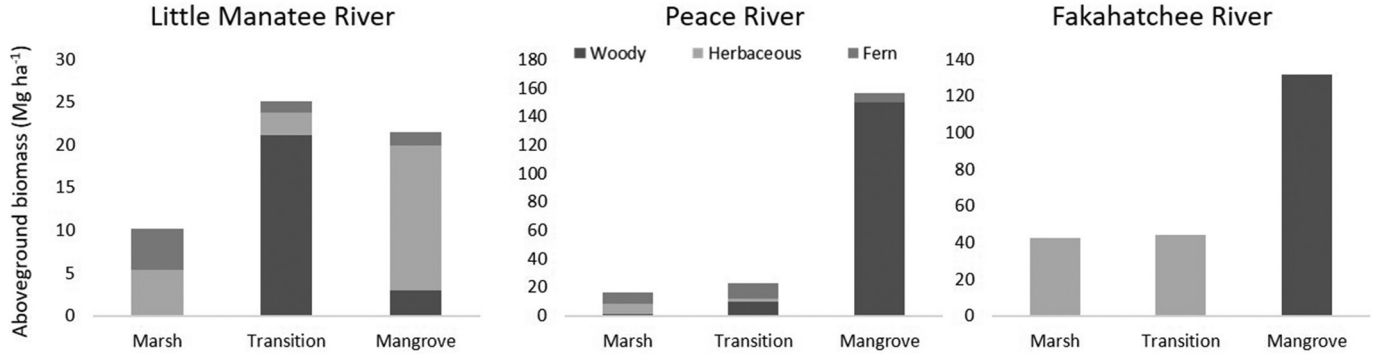

Fig. 2. Biomass distributions (in Mg ha^{-1}) of woody and herbaceous vegetation at each study site. Fern (*Achrostichum danaeifolium*) is separate from herbaceous vegetation and comprises a significant portion of biomass at the Little Manatee River and Peace Rivers.

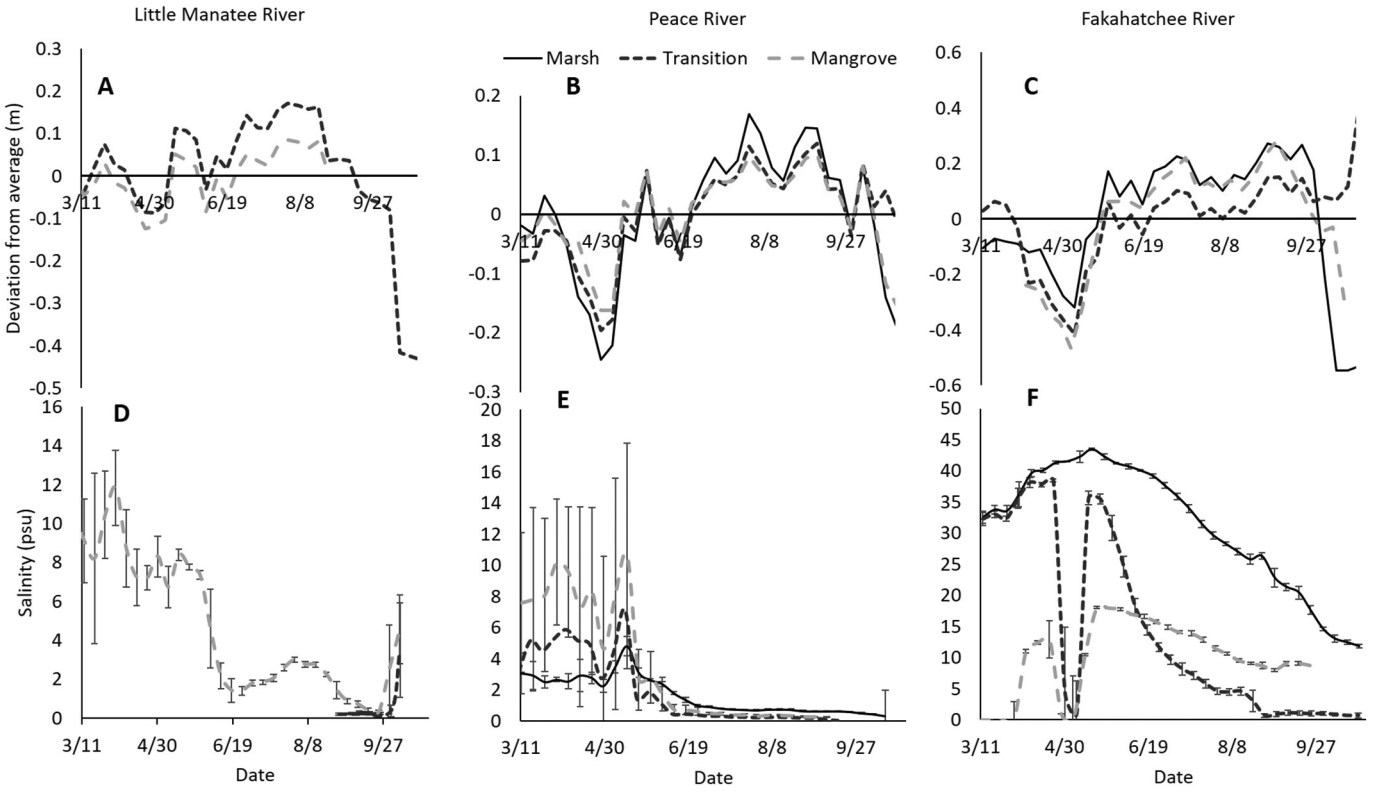

Fig. 3. Deviations from mean annual water level (in meters) (A-C) and mean weekly salinity (in psu) (D–F) for field sites. Error bars are weekly standard deviation. Note different scales on y-axis. For water level, < 0 = dry-down, > 0 = higher than average.

In contrast, salinity in the wet season was lowest at the transition site and highest at the marsh site (Fig. 3F). Surface water concentrations of DOC, NH_4^+, and PO_4^{3-} were similar between sites and seasons. Dry season NO_x^- concentrations were below detection at all sites and increased to 0.05–0.06 mg L^{-1} in the wet season (Supplementary Table 2).

3.2. Biogeochemistry

3.2.1. Soil physicochemical properties

Soil OM was most influenced by river and the interaction between river and site ($F = 77.1$; $p < 0.01$; Table 2). Soil OM concentrations decreased slightly with depth ($F = 19$; $p < 0.01$), and patterns were non-seasonal. Soil OM content was lowest at the Little Manatee and Peace Rivers and greatest at the Fakahatchee River (Table 1; Fig. 4). Soil DBD decreased with added organic matter ($F = 27.6$; $p < 0.001$) and generally increased with depth ($F = 10.8$; $p < 0.001$) (Tables 1 and 2). Organic matter had a strong positive relationship with moisture content ($F = 67.8$; $p < 0.001$; Table 2). Moisture content was non-seasonal and generally decreased with depth ($F = 5.12$; $p < 0.01$). Season had the strongest relationship with soil pH ($F = 26.6$; $p < 0.001$), followed by river ($F = 14.6$; $p < 0.001$; Table 2). pH was higher in the wet season than in the dry season.

Table 1
Physicochemical parameters at sites by river and season. Values are averaged over depth ± SE. If season was a significant term in the model, values are separated by season. Trans. = transition and mang. = mangrove.

River	Site	Season	Dry bulk density (g cm^{-3})	pH	Moisture content (%)	Soil organic matter (g kg^{-1})	Total C (mg kg^{-1})	Total N (mg kg^{-1})	Total P (mg kg^{-1})
Little Manatee	Marsh	Dry	0.29 ± 0.04	6.74 ± 0.1	70.3 ± 2	188 ± 20	107 ± 13	5.7 ± 0.8	1614 ± 144
		Wet	0.27 ± 0.04	7.00 ± 0.08					
	Trans.	Dry	0.64 ± 0.09	7.06 ± 0.09	61.5 ± 2	105 ± 11	57 ± 7	3.1 ± 0.4	1168 ± 92
		Wet	0.33 ± 0.05	7.32 ± 0.08					
	Mang.	Dry	0.81 ± 0.11	7.17 ± 0.09	46.2 ± 2	44 ± 5	26 ± 3	1.1 ± 0.2	887 ± 66
		Wet	0.81 ± 0.11	7.43 ± 0.09					
Peace	Marsh	Dry	0.79 ± 0.11	7.73 ± 0.09	50.8 ± 2	40 ± 4	23 ± 3	1.4 ± 0.2	1231 ± 93
		Wet	0.63 ± 0.09	7.98 ± 0.09					
	Trans.	Dry	0.23 ± 0.03	7.33 ± 0.08	68.1 ± 2	183 ± 19	91 ± 11	6.2 ± 0.8	2549 ± 237
		Wet	0.64 ± 0.09	7.59 ± 0.08					
	Mang.	Dry	0.22 ± 0.03	7.31 ± 0.08	75.4 ± 2	260 ± 28	150 ± 17	6.5 ± 0.8	1619 ± 156
		Wet	0.29 ± 0.04	7.56 ± 0.08					
Faka-hatchee	Marsh	Dry	0.12 ± 0.02	7.81 ± 0.1	68.5 ± 3	659 ± 70	269 ± 43	20.5 ± 3.7	201 ± 70
		Wet	0.14 ± 0.02	8.06 ± 0.11					
	Trans.	Dry	0.14 ± 0.02	7.78 ± 0.1	69.7 ± 3	637 ± 68	282 ± 44	20.5 ± 3.6	466 ± 90
		Wet	0.13 ± 0.02	8.03 ± 0.1					
	Mang.	Dry	0.13 ± 0.02	8.22 ± 0.08	74.9 ± 2	425 ± 45	221 ± 27	15.1 ± 2.1	566 ± 54
		Wet	0.15 ± 0.02	8.47 ± 0.08					

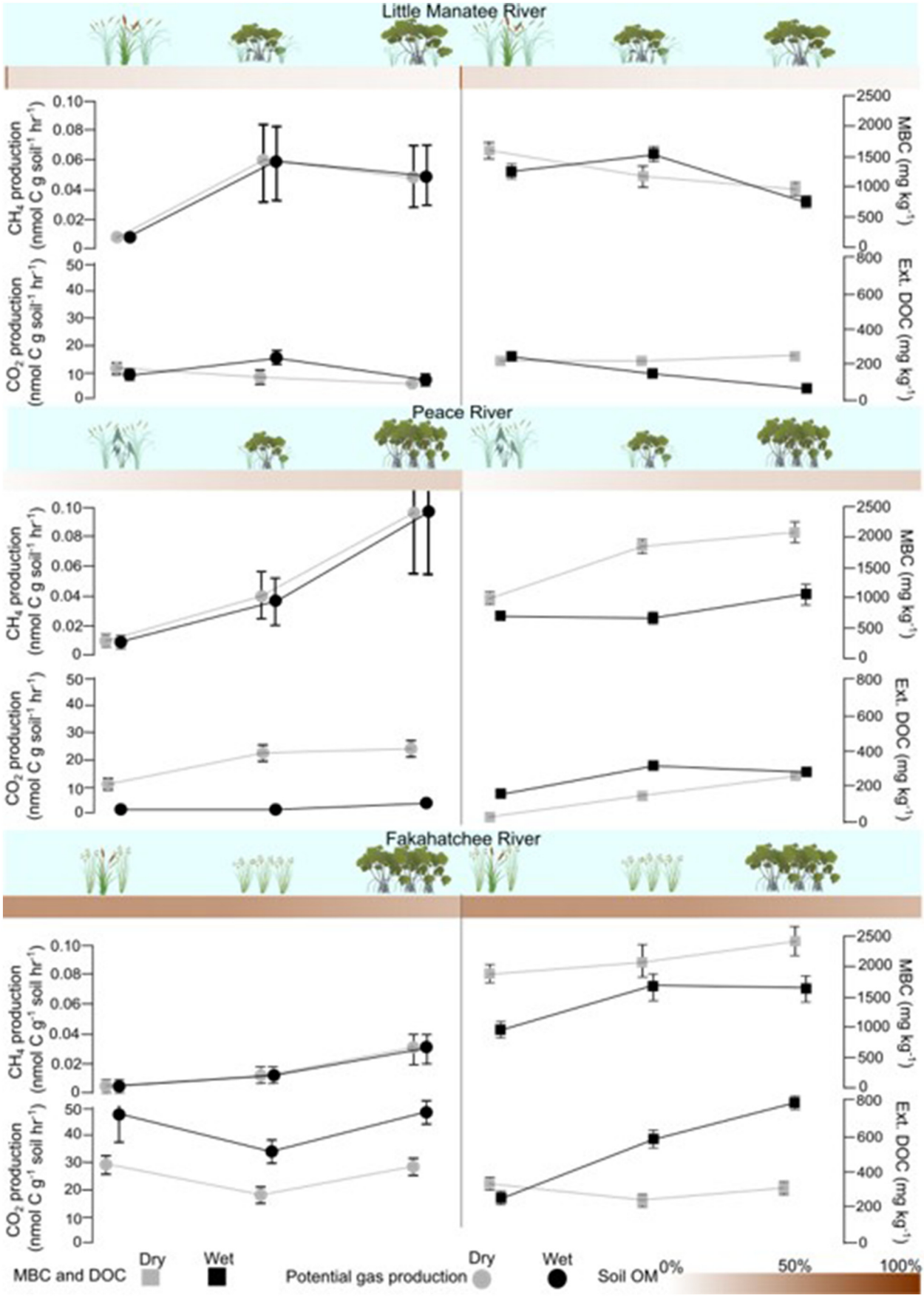

Fig. 4. Clockwise in each panel: mean potential CH_4 production, microbial biomass C, DOC, and potential CO_2 production at all rivers. Gray lines are dry season and black lines are wet season. Data are averaged over depth. Error bars represent standard error. Brown bars are the soil organic matter gradients at each river. (For interpretation of the references to colour in this figure legend, the reader is referred to the web version of this article.)

Table 2
ANCOVA sums-of-squares for all models. Darker shades of gray for each parameter indicate a stronger explanatory power of the individual predictors (soil OM proportion (OMp), River, Site, etc.). Blank cells indicate that the predictor was not used within the model. Italics = $p < 0.05$, bold = $p < 0.01$, bold italics = $p < 0.001$.

Parameter	OMp	River	Site	Depth	Season	River * Site	R^2
Bulk density	***6.9***	***15.8***	***10.3***	***8.07***		***22.8***	0.81
Moisture content	***5990***	***4820***	***7020***	**1360**		***1390***	0.84
pH	***1.83***	***15.1***	***2.49***	*1.05*	***3.34***	***5.58***	0.72
Soil OM		***85.1***	***19***	***9.06***		***77.1***	0.79
Total C	***4.55***	***28.4***	***16***	***13.6***		***46.7***	0.78
Total N	***4.8***	***30.6***	***20.2***	***18.8***		***43.73***	0.78
Total P	***14.3***	***15.9***	***7.98***			***20.5***	0.6
Ext. PO_4^{3-}	0	***169***	0	***433***	***475***	***503***	0.35
Ext. NO_x^-	-87.7	165	11.7	***86***	***478.88***	***15.6***	0.56
Ext. NH_4	0	***1100***	0	0	***1350***	***164***	0.84
Ext. DOC	***8.47***	***12.5***	1.54		*2.43*	***12.4***	0.72
Microbial biomass C	24.86	1.36	2.63		6.42	***6.67***	0.75
Pot. CO_2 production	***35.9***	***8.04***	**4.17**		**3.82**	***9.38***	0.8
Pot. CH_4 production	***195***		***103.14***		0.21		0.12

3.2.2. Total and extractable nutrients

Total C ($F = 18.6$; $p < 0.001$) and N ($F = 20.2$; $p < 0.001$) generally decreased with depth. Soil OM content had a positive relationship with total C ($F = 18.6$; $p < 0.001$) and N ($F = 15.4$; $p < 0.001$) concentrations along all rivers. The Fakahatchee River had the highest average total C and N concentrations out of the three rivers. Soil OM had the strongest relationship with total P concentrations ($F = 58.8$; $p < 0.001$) along with river ($F = 32.7$; $p < 0.001$) and the interaction between river and site ($F = 21.1$; $p < 0.001$). Generally, the Peace River had the highest average total P concentration out of the three rivers studied (Table 1).

All extractable inorganic nutrients were seasonal and had no relationship with soil OM (Table 2). Generally, extractable nutrient concentrations were highest during the dry season (Fig. 5). Neither site alone

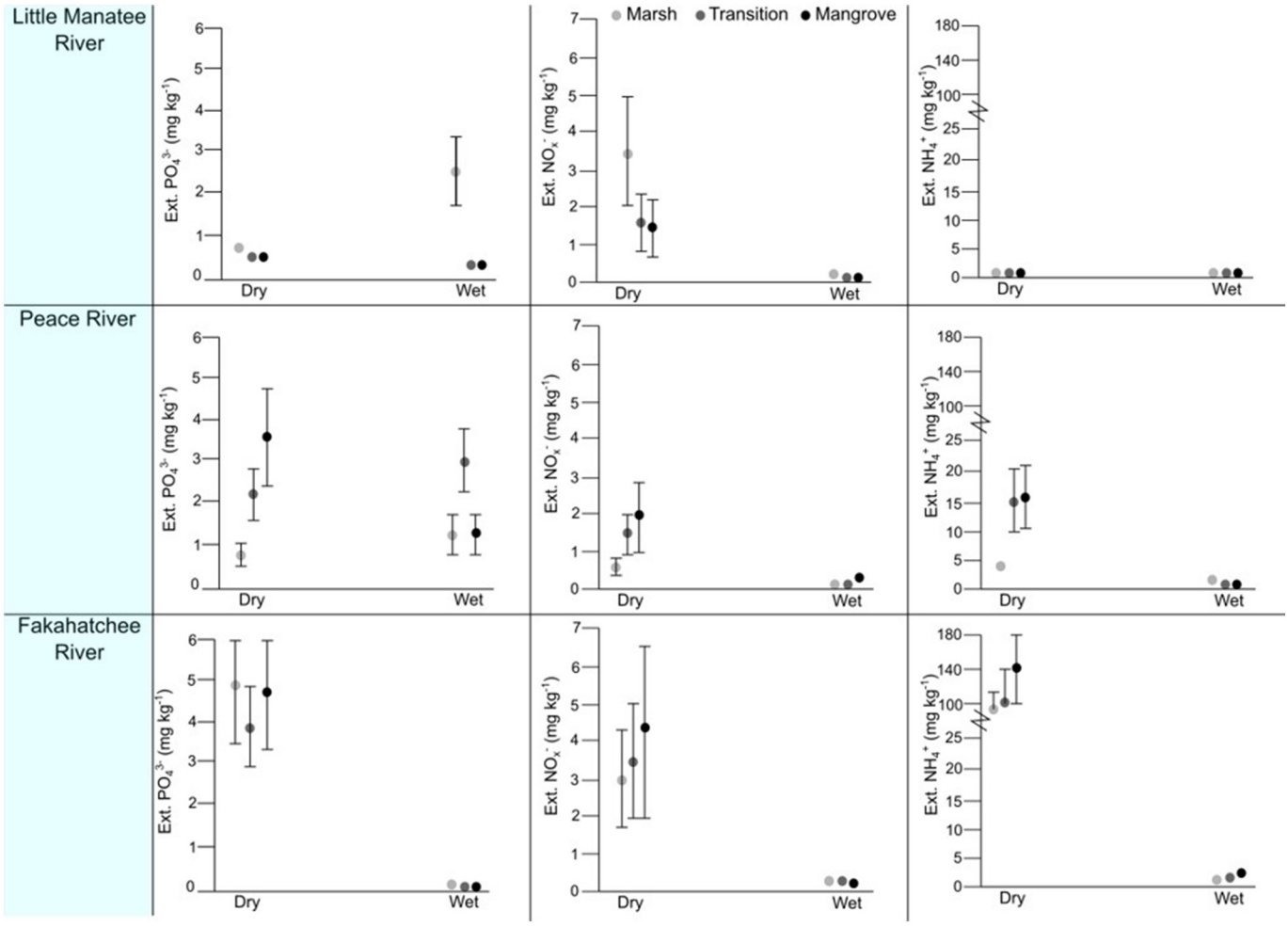

Fig. 5. Extractable nutrients by point and season at all rivers. Marsh sites are in light gray, transition sites are in dark gray, and mangrove sites are in black. Data are averaged over depth. Error bars are standard error.

nor depth determined extractable PO_4^{3-} and the strongest predictor was season ($F = 326$; $p < 0.001$; Table 2). Extractable PO_4^{3-} concentrations increased across the landscape from the Little Manatee River to the Peace and Fakahatchee Rivers. The Little Manatee River marsh site had the highest concentrations during both dry and wet seasons, while the transition and mangrove sites were similar. At the Peace River, extractable PO_4^{3-} concentrations usually increased downstream. The Fakahatchee River was relatively homogenous, with a dry season-low at the transition site to a high at the marsh site. Wet season extractable PO_4^{3-} concentrations were markedly lower and decreased downstream.

Extractable NO_x^- concentrations were highly seasonal ($F = 225$; $p < 0.001$), decreased with depth ($F = 13.5$; $p < 0.001$), and differed by river ($F = 38.9$; $p < 0.001$; Fig. 5; Table 2). Concentrations were up to eight times higher in the dry season than in the wet season (Fig. 5). As with PO_4^{3-}, extractable NO_x^- decreased moving downstream at the Little Manatee River. The Peace River's extractable NO_x^- increased from the marsh to the mangrove site. At the Fakahatchee River, extractable NO_x^- concentrations were generally lowest at the marsh site and peaked at the mangrove site. However, within-site variation was too high to distinguish between sites ($F = 2.75$; $p = 0.07$).

Extractable NH_4^+ concentrations were strongly predicted by season ($F = 1350$; $p < 0.001$) and river ($F = 1100$; $p < 0.001$; Table 2). Sites along the Little Manatee River had consistently low extractable NH_4^+, and this nutrient was detectable only during the dry season. The Peace River marsh site had 75% less extractable NH_4^+ than the transition and mangrove sites during the dry season. Wet season extractable NH_4^+ were above detection for only the marsh site. Overall, the highest concentrations of extractable NH_4^+ were at the Fakahatchee River.

Concentrations of DOC were positively correlated with soil OM ($F = 8.47$; $p < 0.001$), and patterns differed by river ($F = 12.5$; $p < 0.001$) and the interaction between river and site ($F = 12.4$; $p < 0.001$). On the Little Manatee River, concentrations were higher and more similar during the dry season and decreased downstream during the wet season (Fig. 4). However, the pattern was reversed at the Peace and Fakahatchee Rivers, where DOC concentrations were higher during the wet season at most sites and increased downstream. The Peace River's marsh site generally had the lowest DOC concentrations. The transition site was the highest during the wet season, while the mangrove site had the maximum DOC concentration on the river. The Fakahatchee River had the greatest amount of DOC of all three rivers during both seasons. The marsh site had the highest concentration during the dry season. During the wet season, the local minimum was at the marsh site, and the greatest DOC concentration was found at the mangrove site.

3.2.3. Microbial characteristics

Microbial biomass C varied by the interaction between river and site ($F = 6.2$; $p < 0.001$) and was positively related to soil OM ($F = 92.6$; $p < 0.001$; Table 2). Microbial biomass C was generally higher during the dry season ($F = 23.9$; $p < 0.001$; Table 2). The Little Manatee River's mangrove site had the lowest microbial biomass C, irrespective of the season. Dry season microbial biomass C was highest at the marsh site, while wet season concentrations peaked at the transition site. At the Peace River, microbial biomass C increased downstream. The Fakahatchee River had the highest microbial biomass C out of the three rivers. Values were similar between sites during the dry season. However, the marsh site had significantly less microbial biomass C than the transition and mangrove sites during the wet season.

Potential CO_2 production had a strong, positive relationship with soil OM ($F = 86.6$; $p < 0.001$), followed by river ($F = 9.7$; $p < 0.001$) and the interaction between site and river ($F = 9.21$; $p < 0.001$; Table 2). At the Little Manatee River, dry season CO_2 production peaked at the marsh site and was lowest at the mangrove site, while the transition site produced the greatest amount of CO_2 during the wet season. Potential CO_2 production generally increased downstream at the Peace River: the marsh site had the lowest rates during both the dry and wet seasons. At the Fakahatchee River, potential CO_2 production increased from the marsh site to the mangrove site.

Patterns of potential CH_4 production were not differentiated by season or river but generally increased moving downstream ($F = 18.2$; $p < 0.001$) and had a positive relationship with soil OM ($F = 68.8$; $p < 0.001$; Table 2). Along the Little Manatee River, the marsh site produced the least CH_4, and the local maximum was at the transition site. The Peace River's marsh site also had the lowest CH_4 production, but production peaked at the mangrove site. The variation between samples was high, especially for the Peace River's soils (Fig. 4). The Fakahatchee River displayed a similar trend to the Peace River.

3.2.4. Principal component analysis

PC1 and PC2 explained 48.6% and 16.3% of the variation within the data, respectively (Fig. 6). When data were grouped by vegetation community, there was little difference between the sites (Fig. 6a). The marsh and transition sites overlapped slightly more than either did with the mangrove sites, indicating that the former pair were more like each other than to the mangrove sites. In contrast, significant differences in the data were seen when the PCA was grouped by river (Fig. 6b). Rivers separated along PC1. The Fakahatchee River was characterized by greater soil OM, microbial biomass C, greenhouse gas production, total C and N, and extractable NH_4^+. Both the Little Manatee and Peace Rivers separated from the Fakahatchee River via increased soil DBD. The Peace River was an intermediate between the other two rivers, as some sites on the Peace River showed intermediate characteristics compared to the other two rivers. Season structured and separated data along PC2 (Fig. 6c) indicating seasonality has a major influence on biogeochemistry. Extractable DOC, pH, and potential CO_2 and CH_4 production were generally higher in the wet season, while higher concentrations of extractable inorganic nutrients were found in the dry season. The Fakahatchee River's strong seasonality likely drove this trend.

4. Discussion

We predicted dominant vegetation community (marsh vs. mangrove) would serve as a strong predictor of biogeochemical properties and processes. However, the data revealed more nuanced interactions and, at times, contradicted previously established paradigms. Contrary to our initial prediction, coastal wetland soil biogeochemistry patterns were inconsistent from river to river. Season directed inorganic nutrient concentrations more than any other predictor in this study.

4.1. Vegetation community was not a robust indicator of salinity

How different ecosystems transition from one species assemblage to another in response to sea-level rise depends on the individual species' salinity tolerance. Some plants, like *Taxodium distichum* (Krauss et al., 2009) and *Sagittaria lancifolia* (Howard and Mendelssohn, 1999), show reduced growth with salinity as low as 1.3, while others, such as *Scirpus americanus*, have a wide salt tolerance ($0 < S < 12$; Howard and Mendelssohn, 1999). Indeed, *S. americanus* was found at the transition sites on both the Little Manatee and Peace Rivers, which experienced salinity values between <0.5 and approximately 5 (Supplementary Table 2). *Rhizophora mangle* dominated the downstream end-member sites on the Little Manatee and Peace Rivers. However, under the canopy, the biogeochemical characteristics were divergent, despite the similar vegetation community and salinity. Therefore, although mangrove encroachment generally increased aboveground biomass at each location, it was not a direct proxy for abiotic conditions.

The expansion of mangroves into previously freshwater marsh has been linked to saltwater intrusion. While mangroves are typically found in saline and brackish environments, they can also establish in freshwater systems, provided that interspecific competition from other mangroves is low. Howard et al. (2015) found that 62-75% of

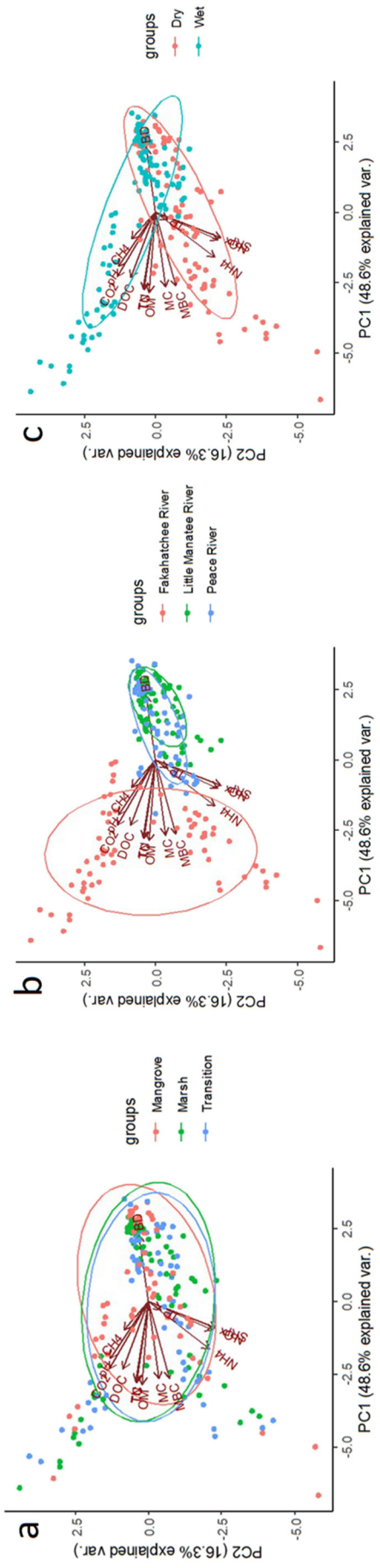

Fig. 6. Principal component analysis of data grouped by site (a), river (b), and season (c).

A. germinans and L. *racemosa* survived in freshwater conditions in greenhouse marsh mesocosm single-species plantings. Mangroves located in mesohaline environments along rivers can continue migrating upstream (Yang et al., 2013). Just one long-lasting storm surge that transports a high density of mangrove propagules can shift a previously freshwater marsh to a mangrove forest, as shown by a modeling study of the marsh-mangrove ecotone in the Everglades (Jiang et al., 2014). An extremely dry year followed by an active hurricane season could be enough to transition the freshwater ecosystem to a mangrove swamp.

Based on previous studies, some may assume that mangroves' landward extent coincides with an abiotic salinity and water level threshold. This study found that the mangrove ecotone (transition site) on the Little Manatee and Peace Rivers occurred where salinity averaged approximately 5 during the dry season. However, weekly average salinity converged as wet season rains fell, and all sites on these two rivers became roughly fresh ($S < 0.6$) from June to September. At the Fakahatchee River during the dry season, saline water ($S > 30$) was detected 8 km inland from the coast at the marsh and transition sites, while the mangrove site remained brackish in April 2018. Salinity began to decrease in late May at all three sites. The Fakahatchee marsh retained the highest local salinity through the end of the sampling period, which could be due to poor hydrologic connectivity between areas north and south of US 41, a known barrier to water movement in the region (Howard et al., 2017; Krauss et al., 2018).

The marsh-mangrove ecotone is not always the location of biogeochemical intermediates. Generally, the marsh and transition sites were more like each other than either was to the mangrove sites, but this distinction is slight (Fig. 6a). This finding opposes previous research, where the transition zone was more functionally similar to the invading mangrove zone in a salt marsh-mangrove ecotone in Merritt Island, Florida (Steinmuller et al., 2020). This contrast could be because our study was conducted along rivers with multiple channels and modifications, not in a marsh expanse, as in Steinmuller et al. (2020). As mangroves migrate inland via river channels, new mangroves establish in soil formed under herbaceous vegetation. In another Merrit Island study, CO_2 flux was consistently lower from mangrove soils planted with mangrove seedings (*A. germinans*; 2.91 μg C m^{-2} s^{-1}) than from vegetation-free marsh soils (developed under *Spartina alterniflora*; 8.18 μg C m^{-2} s^{-1}) in an experimental mesocosm. Furthermore, soil respiration rates were consistently higher in marsh soils, demonstrating that, upon initial mangrove establishment, CO_2 flux may remain elevated until enough mangrove litter accumulates to change the soil structure (Geoghegan et al., 2021). In contrast, *A. germinans* soil consistently released more CO_2-C than *J. roemerianus* soils in field respiration measurements from Tampa Bay, FL (Lewis et al., 2014). Therefore, there may be a lag time between mangrove recruitment and expansion in a previously herbaceous marsh and a quantifiable shift in soil properties due to the new vegetation community.

4.2. Coastal wetland biogeochemical gradients vary across the landscape

Rivers are notoriously variable systems in both time and space (Thoms, 2006). The Little Manatee River was the only location to follow the "classic" coastal wetland soil OM gradient of decreasing OM content with increasing salinity (Chambers et al., 2013; Morrissey et al., 2014; Odum, 1988; Tam and Wong, 1998; Williams et al., 2014; Zhang et al., 2019), with the marsh site having approximately 76% more soil OM than the mangrove site. This river was also the only location with all three sites on the main channel, which may have influenced this trend. However, the mangrove site had the highest soil OM content on the Peace River. Greater boat traffic on the Peace River, both in size and number of boats, may have contributed to increased erosion and soil loss in this system (Mcconchie and Toleman, 2019; Harttung, personal observation). Also, the presence of more mature mangroves on the Peace River may have enhanced the ability of prop roots to act as wave breaks, allowing authigenic OM to accumulate rather than wash

away (Gedan et al., 2011). Finally, there was no gradient in soil OM content along the salinity/vegetation transect at the Fakahatchee River; the river was relatively homogeneous in soil properties in general.

Soil OM was correlated with many biogeochemical parameters, including moisture content, total C, total N, DOC, microbial biomass C, and potential CO_2 production (Fig. 6a-c). Soils high in OM have an enhanced cation exchange capacity compared to other soils, adsorbing high concentrations of nutrients and releasing them through desorption and decomposition (Capone and Kiene, 1988; Puustjärvi, 1956; Tiessen et al., 1994; Wood et al., 2018). As the interaction between site and river was significant in all models, this is evidence that location must be considered when evaluating characteristics of wetland vegetation communities.

4.3. Greenhouse gas production correlates with soil organic matter content across the landscape

The Little Manatee and Peace Rivers displayed opposite patterns of potential CO_2 production, with soil OM explaining the most variation within the model (Table 2). The highly organic mangrove site at the Peace River produced ~3 times more CO_2 than the low soil OM marsh site. At the Little Manatee River, the marsh site's soil contained the most OM, and CO_2 production was ~2 times higher than from the mangrove site's soil. The highly organic soils of the Fakahatchee River had order-of-magnitude greater rates of CO_2 production than either of the other two rivers (Fig. 4). In a comparison of storm surge sediment (primarily mineral) and underlying soils (primarily organic) from the same sites in southwest Florida, OM was similarly positively correlated with greater potential CO_2 production (Breithaupt et al., 2020). Soil OM is a major electron donor for microbial respiration in wetland soils. When OM is limited, any areas of high concentration become microbial activity hotspots (Gallardo and Schlesinger, 1994; Hogberg and Ekblad, 1996; Loeppmann et al., 2016; Schnürer et al., 1985). Within the soils themselves, nonrandom distribution of roots may have contributed to variability in soil respiration rates, as only rhizomes were removed during incubation bottle preparation.

It has been thought that mangrove ecosystems produce negligible CH_4 because of the increased availability of sulfate in brackish and saltwater systems, as sulfate-reducing bacteria can generally outcompete methanogens for substrate (Alongi et al., 2000, 2001; Bartlett et al., 1987; Capone and Kiene, 1988; Kristensen, 2007; Sotomayor et al., 1994). However, all the transition and mangrove sites in this study produced detectable (0.02–0.1 μg C g^{-1} h^{-1}) potential CH_4, similar to or higher than their marsh counterparts, despite salinity in the oligo- to mesohaline range (Fig. 4). This phenomenon is likely because of plentiful soil OM, which was positively correlated with CH_4 production. At both the Little Manatee and Peace Rivers, CH_4 production increased downstream. Methane production was maintained even during the dry season salinity peak at the Fakahatchee River, when salinity reached a maximum of 45 at the marsh, indicating the likely presence of sulfate-free microzones (King and Wiebe, 1980) and the existence of non-competitive substrates (Oremland and Polcin, 1982; Winfrey and Zeikus, 1977). The Little Manatee River's transition site (intermediate salinity) had the maximum CH_4 production among the sites at that river, which has been found in other studies investigating the relationship between salinity and CH_4 production (Poffenbarger et al., 2011). Methane emissions can gradually increase with increasing salinity, until a tipping point between 7 and 10 (Wang et al., 2017), which is a similar range seen at the Little Manatee River during the dry season. In a study examining tidal marshes along an estuarine salinity gradient, the oligohaline site experienced a greater than expected flux of CH_4 during a saltwater intrusion event that increased salinity to around 5.5 (Weston et al., 2014). These results support the idea that factors other than salinity, such as soil OM, can significantly control methanogenesis (Bartlett et al., 1987; Sjögersten et al., 2016; Sotomayor et al., 1994).

4.4. Seasonality and relationships with inorganic nutrient availability and CO_2 flux

Soil extractable nutrient concentrations from all rivers were lower in the wet season across vegetation communities. Wet season concentrations of extractable inorganic nutrients were lower by 87–100% (NO_x^-), 71–100% (NH_4^+), and 94–100% (PO_4^{3-}) relative to the dry season. This seasonal pattern could be caused by flushing and dilution during the wet season from Florida's daily heavy rains (Misra et al., 2018) and by increased plant uptake due to co-occurrence with the growing season (Jonasson and Chapin, 1991; Lee et al., 2013; Picard et al., 2005; Reddy et al., 2000). The relationship between seasonality and surface water nutrients was strong, albeit inconsistently across rivers. NO_x^- dominated the speciation of dissolved inorganic N in the Little Manatee River's surface water in the wet season, while NH_4^+ was more abundant in the dry season. Increased flow (and less stagnation) during the season of high rainfall and the flux of NH_4^+ from the soil into the water column with heightened dry season salinity could explain this observation (Jun et al., 2013; Luo et al., 2019; Steinmuller and Chambers, 2018; Weston et al., 2010). However, the Peace River's surface waters, representing the largest river with the greatest flow, remained dominated by NO_x^- year-round. Meanwhile, the Fakahatchee River, a shallow, sheet-flow system, had higher NH_4^+ than NO_x^- in surface water year-round. The dominance of NO_x^- at the Peace River and NH_4^+ at the Fakahatchee River could be related to oxygen availability, as outlined above, as fast-flowing water contains more oxygen than slow or stagnant water (House, 2003).

Concentrations of PO_4^{3-} in surface water doubled from the dry to the wet season at the Little Manatee River. Exceptionally high year-round surface water PO_4^{3-} concentrations (~0.5 mg L^{-1}) were found at the Peace River, where phosphate is naturally plentiful and supports intensive mining activities within this watershed (Filippelli, 2011; Zhang and Ross, 2015). Extractable PO_4^{3-} concentrations at the Fakahatchee River were elevated during the dry season, coinciding with a spike in salinity to ~34 at the "freshwater" marsh, possibly due to the intrusion of ocean water or phosphate desorption from soil particles (Boyer, 2006; Paludan and Morris, 1999; Sundareshwar and Morris, 1999).

The Peace River and the Fakahatchee River also showed seasonal variation in CO_2 production but in opposite directions. Generally, CO_2 production increases with oxygen availability, such as during low water periods (Chambers et al., 2013, 2014), as was seen at the Peace River. The Fakahatchee River, on the other hand, had higher CO_2 production during the wet season when water levels were at their highest, which may be due to the extreme saltwater-intrusion event that occurred during the dry season. In this case, the dry season salinity was so high that the additional H_2S produced during sulfate reduction and abundance of Cl^- may have stressed the microbial and vegetation communities and reduced metabolic activity (Howes et al., 1981; Lamers et al., 2013; McKee and Mendelssohn, 1989; Mirzoyan and Schreier, 2014; Rath and Rousk, 2015).

5. Conclusion

The most consistent correlate of biogeochemical properties and processes across all three coastal riverine wetlands studied was soil OM content, more so than salinity, plant biomass, or vegetation community (marsh vs. mangrove). This study highlights the high degree of variability among coastal riverine wetland ecosystems, even within a narrow geographic area, and the importance of site-specific investigations over relying on general patterns observed within the literature. Specifically, this study found that 1) soil OM does not always decline across the gradient from freshwater tidal marshes to saltwater mangroves, 2) the vegetation ecotone (transition zone) is not necessarily the site of biogeochemical intermediates (e.g., the transition was more similar to the marsh at the Little Manatee and Fakahatchee Rivers and the mangrove at the Peace River), and 3) methane production can be

highest in mangrove/saline vegetation communities if soil OM content is high. Moreover, the location of the mangrove ecotone does not appear to reflect a specific salinity tipping point. Instead, salinity is dynamic over seasons, with the ecotone being characterized as fresh ($S < 0.5$) during most of the wet season at all sites and ranging widely ($5 < S <$ ~45) during the dry season. Instead of focusing on vegetation communities, we suggest that a simple investigation of soil OM content across a wetland salinity gradient of interest will be the best indicator of various ecologically important biogeochemical properties, including nutrient storage availability and cycling, and greenhouse gas production.

CRediT authorship contribution statement

Sarah A. Harttung: conceptualization; data curation; software; formal analysis; investigation; methodology; visualization; writing - original draft; writing - review & editing;

Kara R. Radabaugh: data curation; investigation; methodology; writing - review & editing

Ryan P. Moyer: data curation; investigation; methodology; writing - review & editing

Joseph M. Smoak: funding acquisition; writing - review & editing

Lisa G. Chambers: conceptualization; funding acquisition; project administration; resources; supervision; original draft; writing - review & editing

Declaration of competing interest

The authors declare that they have no known competing financial interests or personal relationships that could have appeared to influence the work reported in this paper.

Acknowledgments

This work is supported by Interagency Climate Change NASA program grant no. 2017-67003-26482/project accession no. 1012260 from the USDA National Institute of Food and Agriculture. Field and laboratory work for biogeochemical properties and processes would not have been possible without the assistance of members of the Aquatic Biogeochemistry Lab at the University of Central Florida (Ashley Boggs, Angela Ferebee, Chelsea Nitsch, Paul Boudreau, and Havalend Steinmuller) and Audrey Goeckner. Field and laboratory efforts for vegetation characterization were assisted by Amanda Chappel, Emma Dontis, Christine Russo, Carey Schafer, Emma Wennick, and Sam Roussopoulos. We would also like to acknowledge the input and feedback of Brad Rosenheim and David Lagomasino on the overall research project.

Appendix A. Supplementary data

Supplementary data to this article can be found online at https://doi.org/10.1016/j.scitotenv.2021.149056.

References

Alongi, D.M., Tirendi, F., Trott, L.A., Xuan, T.T., 2000. Benthic decomposition rates and pathways in plantations of the mangrove Rhizophora apiculata in the Mekong delta, Vietnam. Mar. Ecol. Prog. Ser. 194, 87–101. https://doi.org/10.3354/meps194087.

Alongi, D.M.M., Wattayakorn, G., Pfitzner, J., Tirendi, F., Zagorskis, I., Brunskill, G.J.J., Davidson, A., Clough, B.F.F., 2001. Organic carbon accumulation and metabolic pathways in sediments of mangrove forests in southern Thailand. Mar. Geol. 179, 85–103. https://doi.org/10.1016/S0025-3227(01)00195-5.

Andersen, J.M., 1976. An ignition method for determination of total phosphorous in lake sediments. Water Res. 10, 329–331. https://doi.org/10.1016/0043-1354(76)90175-5.

Ball, M.C., 1988. Ecophysiology of mangroves. Trees 2, 129–142. https://doi.org/10.1007/BF00196018.

Barbier, E.B., Hacker, S.D., Kennedy, C., Koch, E.W., Stier, A.C., Silliman, B.R., 2011. The value of estuarine and coastal ecosystem services. Ecol. Monogr. 81, 169–193. https://doi.org/10.1890/10-1510.1.

Bartlett, K.B., Bartlett, D.S., Harriss, R.C., Sebacher, D.I., 1987. Methane emissions along a salt marsh salinity gradient. Biogeochemistry 4, 183–202. https://doi.org/10.1007/BF02187365.

Boyer, J.N., 2006. Shifting N and P limitation along a north-south gradient of mangrove estuaries in South Florida. Hydrobiologia 569, 167–177. https://doi.org/10.1007/s10750-006-0130-3.

Breithaupt, J.L., Hurst, N., Steinmuller, H.E., Duga, E., Smoak, J.M., Kominoski, J.S., Chambers, L.G., 2020. Comparing the biogeochemistry of storm surge sediments and pre-storm soils in coastal wetlands: hurricane Irma and the Florida Everglades. Estuar. Coasts 43, 1090–1103. https://doi.org/10.1007/s12237-019-00607-0.

Capone, D.G., Kiene, R.P., 1988. Comparison of microbial dynamics in marine and freshwater sediments: contrasts in anaerobic carbon catabolism. Limnol. Oceanogr. 33, 725–749. https://doi.org/10.4319/lo.1988.33.4part2.0725.

Cavanaugh, K.C., Kellner, J.R., Forde, A.J., Gruner, D.S., Parker, J.D., Rodriguez, W., Feller, I.C., 2014. Poleward expansion of mangroves is a threshold response to decreased frequency of extreme cold events. Proc. Natl. Acad. Sci. 111, 723–727. https://doi.org/10.1073/pnas.1315800111.

Chambers, L.G., Reddy, K.R., Osborne, T.Z., 2011. Short-term response of carbon cycling to salinity pulses in a freshwater wetland. Soil Sci. Soc. Am. J. 75, 2000–2007. https://doi.org/10.2136/sssaj2011.0026.

Chambers, L.G., Osborne, T.Z., Reddy, K.R., 2013. Effect of salinity-altering pulsing events on soil organic carbon loss along an intertidal wetland gradient: a laboratory experiment. Biogeochemistry 115, 363–383. https://doi.org/10.1007/s10533-013-9841-5.

Chambers, L.G., Davis, S.E., Troxler, T., Boyer, J.N., Downey-Wall, A., Scinto, L.J., 2014. Biogeochemical effects of simulated sea level rise on carbon loss in an Everglades mangrove peat soil. Hydrobiologia 726, 195–211. https://doi.org/10.1007/s10750-013-1764-6.

Coldren, G.A., Langley, J.A., Feller, I.C., Chapman, S.K., 2019. Warming accelerates mangrove expansion and surface elevation gain in a subtropical wetland. J. Ecol. 107, 79–90. https://doi.org/10.1111/1365-2745.13049.

Conner, W.H., McLeod, K.W., McCarron, J.K., 1997. Flooding and salinity effects on growth and survival of four common forested wetland species. Wetl. Ecol. Manag. 5, 99–109. https://doi.org/10.1023/A:1008251127131.

Costanza, R., D'Arge, R., de Groot, R., Farber, S., Grasso, M., Hannon, B., Limburg, K., Naeem, S., O'Neill, R.V., Paruelo, J., Raskin, R.G., Sutton, P., van den Belt, M., 1998. The value of the world's ecosystem services and natural capital. Nature 387, 253–260. https://doi.org/10.1038/387253a0.

Craft, C., 2007. Freshwater input structures soil properties, vertical accretion, and nutrient accumulation of Georgia and U.S. tidal marshes. Limnol. Oceanogr. 52, 1220–1230. https://doi.org/10.4319/lo.2007.52.3.1220.

Craft, C.B.B., Seneca, E.D.D., Broome, S.W.W., 1991. Loss on ignition and kjeldahl digestion for estimating organic carbon and total nitrogen in estuarine marsh soils: calibration with dry combustion. Estuaries 14, 175–179. https://doi.org/10.2307/1351691.

Delignette-Muller, M.L., Dutang, C., 2015. An R package for fitting distributions. J. Stat. Softw. 64, 1–34. https://doi.org/10.18637/jss.v064.i04.

Edmonds, J.W., Weston, N.B., Joye, S.B., Mou, X., Moran, M.A., 2009. Microbial community response to seawater amendment in low-salinity tidal sediments. Microb. Ecol. 58, 558–568. https://doi.org/10.1007/s00248-009-9556-2.

Eslami-Andargoli, L., Dale, P., Sipe, N., Chaseling, J., 2009. Mangrove expansion and rainfall patterns in Moreton Bay, Southeast Queensland, Australia. Estuar. Coast. Shelf Sci. 85, 292–298. https://doi.org/10.1016/j.ecss.2009.08.011.

Filippelli, G.M., 2011. Phosphate rock formation and marine phosphorus geochemistry: the deep time perspective. Chemosphere 84, 759–766. https://doi.org/10.1016/j.chemosphere.2011.02.019.

Gallardo, A., Schlesinger, W.H., 1994. Factors limiting microbial biomass in the mineral soil and forest floor of a warm-temperate forest. Soil Biol. Biochem. 26, 1409–1415.

Gedan, K.B., Kirwan, M.L., Wolanski, E., Barbier, E.B., Silliman, B.R., 2011. The present and future role of coastal wetland vegetation in protecting shorelines: answering recent challenges to the paradigm. Clim. Chang. 106, 7–29. https://doi.org/10.1007/s10584-010-0003-7.

Geoghegan, E.K., Langley, J.A., Chapman, S.K., 2021. A comparison of mangrove and marsh influences on soil respiration rates: a mesocosm study. Estuar. Coast. Shelf Sci. 248, 106877. https://doi.org/10.1016/j.ecss.2020.106877.

Giri, C., Long, J., 2016. Is the geographic range of mangrove forests in the conterminous United States really expanding? Sensors 16, 2010. https://doi.org/10.3390/s16122010.

Hackney, C.T., Avery, G.B., 2015. Tidal wetland community response to varying levels of flooding by saline water. Wetlands 35, 227–236. https://doi.org/10.1007/s13157-014-0597-z.

Helton, A.M., Bernhardt, E.S., Fedders, A., 2014. Biogeochemical regime shifts in coastal landscapes: the contrasting effects of saltwater incursion and agricultural pollution on greenhouse gas emissions from a freshwater wetland. Biogeochemistry 120, 133–147. https://doi.org/10.1007/s10533-014-9986-x.

Herbert, E.R., Boon, P., Burgin, A.J., Neubauer, S.C., Franklin, R.B., Ardon, M., Hopfensperger, K.N., Lamers, L.P.M., Gell, P., Langley, J.A., 2015. A global perspective on wetland salinization: ecological consequences of a growing threat to freshwater wetlands. Ecosphere 6, 1–43. https://doi.org/10.1890/ES14-00534.1.

Hogberg, P., Ekblad, A., 1996. Substrate-induced respiration measured in situ in a C3-plant ecosystem using additions of C4-sucrose. Soil Biol. Biochem. 28, 1131–1138.

House, W.A., 2003. Factors influencing the extent and development of the oxic zone in sediments. Biogeochemistry 63, 317–334. https://doi.org/10.1023/A:1023353318856.

Howard, R.J., Mendelssohn, I.A., 1999. Salinity as a constraint on growth of oligohaline marsh macrophytes. I. Species variation in stress tolerance. Am. J. Bot. 86, 785–794. https://doi.org/10.2307/2656700.

Howard, R.J., Krauss, K.W., Cormier, N., Day, R.H., Biagas, J., Allain, L., 2015. Plant-plant interactions in a subtropical mangrove-to-marsh transition zone: effects of environmental drivers. J. Veg. Sci. 26, 1198–1211. https://doi.org/10.1111/jvs.12309.

Howard, R.J., Day, R.H., Krauss, K.W., From, A.S., Allain, L., Cormier, N., 2017. Hydrologic restoration in a dynamic subtropical mangrove-to-marsh ecotone. Restor. Ecol. 25, 471–482. https://doi.org/10.1111/rec.12452.

Howes, B.L., Howarth, R.W., Teal, J.M., Valiela, I., 1981. Oxidation-reduction potentials in a salt marsh: spatial patterns and interactions with primary production. Limnol. Oceanogr. 26, 350–360. https://doi.org/10.4319/lo.1981.26.2.0350.

Jiang, J., DeAngelis, D.L., Anderson, G.H., Smith, T.J., 2014. Analysis and simulation of propagule dispersal and salinity intrusion from storm surge on the movement of a marsh-mangrove ecotone in South Florida. Estuar. Coasts 37, 24–35. https://doi.org/10.1007/s12237-013-9666-4.

Jonasson, S., Chapin, F.S.I., 1991. Seasonal uptake and allocation of phosphorus in Eriophorum vaginatum L measured by labelling with 32P. New Phytol. 118, 349–357. https://doi.org/10.1111/j.1469-8137.1991.tb00987.x.

Jun, M., Altor, A.E., Craft, C.B., 2013. Effects of increased salinity and inundation on inorganic nitrogen exchange and phosphorus sorption by tidal freshwater floodplain forest soils, Georgia (USA). Estuar. Coasts 36, 508–518. https://doi.org/10.1007/s12237-012-9499-6.

Kelleway, J.J., Saintilan, N., Macreadie, P.I., Skilbeck, C.G., Zawadzki, A., Ralph, P.J., 2016. Seventy years of continuous encroachment substantially increases "blue carbon" capacity as mangroves replace intertidal salt marshes. Glob. Chang. Biol. 22, 1097–1109. https://doi.org/10.1111/gcb.13158.

King, G.M., Wiebe, W.J., 1980. Regulation of sulfate concentrations and methanogenesis in salt marsh soils. Estuar. Coast. Mar. Sci. 10, 215–223. https://doi.org/10.1016/S0302-3524(80)80059-4.

Koretsky, C.M., Van Cappellen, P., DiChristina, T.J., Kostka, J.E., Lowe, K.L., Moore, C.M., Roychoudhury, A., Viollier, E., 2005. Salt marsh pore water geochemistry does not correlate with microbial community structure. Estuar. Coast. Shelf Sci. 62, 233–251. https://doi.org/10.1016/j.ecss.2004.09.001.

Kostka, J.E., Roychoudhury, A., Van Cappellen, P., 2002. Rates and controls of anaerobic microbial respiration across spatial and temporal gradients in saltmarsh sediments. Biogeochemistry 60, 49–76. https://doi.org/10.1023/A:1016525216426.

Krauss, K.W., Duberstein, J.A., Doyle, T.W., Conner, W.H., Day, R.H., Inabinette, L.W., Whitbeck, J.L., 2009. Site condition, structure, and growth of baldcypress along tidal/non-tidal salinity gradients. Wetlands 29, 505–519. https://doi.org/10.1672/08-77.1.

Krauss, K.W., From, A.S., Doyle, T.W., Doyle, T.J., Barry, M.J., 2011. Sea-level rise and landscape change influence mangrove encroachment onto marsh in the Ten Thousand Islands region of Florida, USA. J. Coast. Conserv. 15, 629–638. https://doi.org/10.1007/s11852-011-0153-4.

Krauss, K.W., Demopoulos, A.W.J., Cormier, N., From, A.S., McClain-Counts, J.P., Lewis, R.R., 2018. Ghost forests of Marco Island: mangrove mortality driven by belowground soil structural shifts during tidal hydrologic alteration. Estuar. Coast. Shelf Sci. 212, 51–62. https://doi.org/10.1016/j.ecss.2018.06.026.

Kristensen, E., 2007. Carbon balance in mangrove sediments: the driving processes and their controls. Greenh. Gas Carbon Balanc. Mangrove Coast. Ecosyst, pp. 61–78.

Lamers, L.P.M., Govers, L.L., Janssen, I.C.J.M., Geurts, J.J.M., Van der Welle, M.E.W., Van Katwijk, M.M., Van der Heid, T., Roelofs, J.G.M., Smolders, A.J.P., 2013. Sulfide as a soil phytotoxin-a review. Front. Plant Sci. 4, 1–14. https://doi.org/10.3389/fpls.2013.00268.

Lee, S.Y., Maniquiz, M.C., Choi, J.Y., Jeong, S.M., Kim, L.H., 2013. Seasonal nutrient uptake of plant biomass in a constructed wetland treating piggery wastewater effluent. Water Sci. Technol. 67, 1317–1323. https://doi.org/10.2166/wst.2013.002.

Lewis, E.L., 1980. The practical salinity scale 1978 and its antecedents. IEEE J. Ocean. Eng. OE-5 (1), 3–8. https://doi.org/10.1109/JOE.1980.1145448.

Lewis, D.B., Brown, J.A., Jimenez, K.L., 2014. Effects of flooding and warming on soil organic matter mineralization in Avicennia germinans mangrove forests and Juncus roemerianus salt marshes. Estuar. Coast. Shelf Sci. 139, 11–19. https://doi.org/10.1016/j.ecss.2013.12.032.

Liu, T., Tao, Y., Liu, Y., 2017. Mangrove swamp expansion controlled by climate since 1988: a case study in the Nanliu River Estuary, Guangxi, Southwest China. Acta Oceanol. Sin. 36, 11–17. https://doi.org/10.1007/s13131-017-1097-9.

Livesley, S.J., Andrusiak, S.M., 2012. Temperate mangrove and salt marsh sediments are a small methane and nitrous oxide source but important carbon store. Estuar. Coast. Shelf Sci. 97, 19–27. https://doi.org/10.1016/j.ecss.2011.11.002.

Loeppmann, S., Blagodatskaya, E., Pausch, J., Kuzyakov, Y., 2016. Enzyme properties down the soil profile - a matter of substrate quality in rhizosphere and detritusphere. Soil Biol. Biochem. 103, 274–283. https://doi.org/10.1016/j.soilbio.2016.08.023.

Loomis, M.J., Craft, C.B., 2010. Carbon sequestration and nutrient (nitrogen, phosphorus) accumulation in river-dominated tidal marshes, Georgia, USA. Soil Sci. Soc. Am. J. 74, 1028. https://doi.org/10.2136/sssaj2009.0171.

Luo, M., Huang, J.F., Zhu, W.F., Tong, C., 2019. Impacts of increasing salinity and inundation on rates and pathways of organic carbon mineralization in tidal wetlands: a review. Hydrobiologia 827, 31–49. https://doi.org/10.1007/s10750-017-3416-8.

Mcconchie, A.J.A., Toleman, I.E.J., 2019. Boat wakes as a cause of riverbank erosion: a case study from the Waikato River, New Zealand. J. Hydrol. 42, 163–179.

McKee, K.L., Mendelssohn, I.A., 1989. Response of a freshwater marsh plant community to increased salinity and increased water level. Aquat. Bot. 34, 301–316. https://doi.org/10.1016/0304-3770(89)90074-0.

Methods for the Determination of Inorganic Substances in Environmental Samples, USEPA 600/R 93/100, August 1993: Method 365.1, Revision 2.0.

Mirzoyan, N., Schreier, H.J., 2014. Effect of sulfide on growth of marine bacteria. Arch. Microbiol. 196, 279–287. https://doi.org/10.1007/s00203-014-0968-0.

Misra, V., Bhardwaj, A., Mishra, A., 2018. Characterizing the rainy season of peninsular Florida. Clim. Dyn. 51, 2157–2167. https://doi.org/10.1007/s00382-017-4005-2.

Morrissey, E.M., Gillespie, J.L., Morina, J.C., Franklin, R.B., 2014. Salinity affects microbial activity and soil organic matter content in tidal wetlands. Glob. Chang. Biol. 20, 1351–1362. https://doi.org/10.1111/gcb.12431.

Neubauer, S.C., 2013. Ecosystem responses of a tidal freshwater marsh experiencing saltwater intrusion and altered hydrology. Estuar. Coasts 36, 491–507. https://doi.org/10.1007/s12237-011-9455-x.

Neubauer, S.C., Franklin, R.B., Berrier, D.J., 2013. Saltwater intrusion into tidal freshwater marshes alters the biogeochemical processing of organic carbon. Biogeosciences 10, 8171–8183. https://doi.org/10.5194/bg-10-8171-2013.

Odum, W.E., 1988. Comparative ecology of tidal freshwater and salt marshes. Annu. Rev. Ecol. Syst. 19, 147–176. https://doi.org/10.1146/annurev.es.19.110188.001051.

Oremland, R.S., Polcin, S., 1982. Methanogenesis and sulfate reduction: competitive and noncompetitive substrates in estuarine sediments. Appl. Environ. Microbiol. 44, 1270–1276. https://doi.org/10.1128/aem.44.6.1270-1276.1982.

Paludan, C., Morris, J.T., 1999. Distribution and speciation of phosphorus along a salinity gradient in intertidal marsh sediments. Biogeochemistry 45, 197–221. https://doi.org/10.1023/A:1006136621465.

Picard, C.R., Fraser, L.H., Steer, D., 2005. The interacting effects of temperature and plant community type on nutrient removal in wetland microcosms. Bioresour. Technol. 96, 1039–1047. https://doi.org/10.1016/j.biortech.2004.09.007.

Poffenbarger, H.J., Needelman, B.A., Megonigal, J.P., 2011. Salinity influence on methane emissions from tidal marshes. Wetlands 31, 831–842. https://doi.org/10.1007/s13157-011-0197-0.

Purvaja, R., Ramesh, R., Frenzel, P., 2004. Plant-mediated methane emission from an indian mangrove. Glob. Chang. Biol. 10, 1825–1834. https://doi.org/10.1111/j.1365-2486.2004.00834.x.

Puustjärvi, V., 1956. On the cation exchange capacity of peats and on the factors of influence upon its formation. Acta Agric. Scand. 6, 410–449. https://doi.org/10.1080/00015125609438024.

Radabaugh, K.R., Moyer, R.P., Chappel, A.R., Powell, C.E., Bociu, I., Clark, B.C., Smoak, J.M., 2018. Coastal blue carbon assessment of mangroves, salt marshes, and salt barrens in Tampa Bay, Florida, USA. Estuar. Coasts 41, 1496–1510. https://doi.org/10.1007/s12237-017-0362-7.

Rath, K.M., Rousk, J., 2015. Salt effects on the soil microbial decomposer community and their role in organic carbon cycling: a review. Soil Biol. Biochem. 81, 108–123. https://doi.org/10.1016/j.soilbio.2014.11.001.

RCoreTeam, 2019. R: A Language and Environment for Statistical Computing.

Reddy, K.R., D'Angelo, E.M., Harris, W.G., 2000. Biogeochemistry of wetlands. In: Sumner, M.E. (Ed.), Handbook of Soil Science (pp. G89-119).

Reid, D.F., 2011. Conversion of specific gravity to salinity for ballast water regulatory management. Ballast Water Management: Combating Aquatic Invaders (Ann Arbor, MI).

RStudioTeam, 2020. RStudio: Integrated Development Environment for R.

Schnürer, J., Clarholm, M., Rosswall, T., 1985. Microbial biomass and activity in an agricultural soil with different organic matter contents. Soil Biol. Biochem. 17, 611–618. https://doi.org/10.1016/0038-0717(85)90036-7.

Sjögersten, S., Caul, S., Daniell, T.J., Jurd, A.P.S., O'Sullivan, O.S., Stapleton, C.S., Titman, J.J., 2016. Organic matter chemistry controls greenhouse gas emissions from permafrost peatlands. Soil Biol. Biochem. 98, 42–53. https://doi.org/10.1016/j.soilbio.2016.03.016.

Sotomayor, D., Corredor, J.E., Morell, J.M., 1994. Methane flux from mangrove sediments along the southwestern coast of Puerto Rico. Estuaries 17, 140–147. https://doi.org/10.2307/1352563.

Spalding, E.A., Hester, M.W., 2007. Interactive effects of hydrology and salinity on oligohaline plant species productivity: implications of relative sea-level rise. Estuar. Coasts 30, 214–225. https://doi.org/10.1007/BF02700165.

Steinmuller, H.E., Chambers, L.G., 2018. Can saltwater intrusion accelerate nutrient export from freshwater wetland soils? An experimental approach. Soil Sci. Soc. Am. J. 82, 283–292. https://doi.org/10.2136/sssaj2017.05.0162.

Steinmuller, H.E., Foster, T.E., Boudreau, P., Ross Hinkle, C., Chambers, L.G., 2020. Tipping points in the mangrove march: characterization of biogeochemical cycling along the mangrove–salt marsh ecotone. Ecosystems 23, 417–434. https://doi.org/10.1007/s10021-019-00411-8.

Sun, B., Cui, L., Li, W., Kang, X., Pan, X., Lei, Y., 2018. A meta-analysis of coastal wetland ecosystem services in Liaoning Province, China. Estuar. Coast. Shelf Sci. 200, 349–358. https://doi.org/10.1016/j.ecss.2017.11.006.

Sundareshwar, P.V., Morris, J.T., 1999. Phosphorus sorption characteristics of intertidal marsh sediments along an estuarine salinity gradient. Limnol. Oceanogr. 44, 1693–1701. https://doi.org/10.4319/lo.1999.44.7.1693.

Tam, N.F.Y., Wong, Y.S., 1998. Variations of soil nutrient and organic matter content in a subtropical mangrove ecosystem. Water Air Soil Pollut. 103, 245–261. https://doi.org/10.1023/A:1004925700931.

Thomas, G.W., 1996. Chapter 16. In: Sparks, D.L., Page, A.L., Helmke, P.A., Loeppert, R.H., Soltanpour, P.N., Tabatabai, M.A., Johnston, C.T., Sumner, M.E. (Eds.), Methods of Soil Analysis Part 3: Chemical Methods. Soil Science Society of America, Inc., Madison, WI, pp. 475–476.

Thoms, M.C., 2006. Variability in riverine ecosystems. River Res. Appl. 22, 115–121. https://doi.org/10.1002/rra.900.

Tiessen, H., Cuevas, E., Chacon, P., 1994. The role of soil organic matter in sustaining soil fertility. Nature 371, 783–785. https://doi.org/10.1038/371783a0.

Twilley, R.R., Chen, R., 1999. A simulation model of organic matter and nutrient accumulation in mangrove wetland soils. Biogeochemistry 44, 93–118. https://doi.org/10.1007/BF00993000.

Vance, E.D., Brookes, P.C., Jenkinson, D.S., 1987. An extraction method for measuring soil microbial biomass C. Soil Biol. Biochem. 19, 703–707. https://doi.org/10.1016/0038-0717(87)90052-6.

Wang, C., Tong, C., Chambers, L.G., Liu, X., 2017. Identifying the salinity thresholds that impact greenhouse gas production in subtropical tidal freshwater marsh soils. Wetlands 37, 559–571. https://doi.org/10.1007/s13157-017-0890-8.

Weiss, R.F., 1974. Carbon dioxide in water and seawater: the solubility of a non-ideal gas. Mar. Chem. 2, 203–215. https://doi.org/10.1016/0304-4203(74)90015-2.

Weston, N.B., Dixon, R.E., Joye, S.B., 2006. Ramifications of increased salinity in tidal freshwater sediments: geochemistry and microbial pathways of organic matter mineralization. J. Geophys. Res. Biogeosci. 111, 1–14. https://doi.org/10.1029/2005JG000071.

Weston, N.B., Giblin, A.E., Banta, G.T., Hopkinson, C.S., Tucker, J., 2010. The effects of varying salinity on ammonium exchange in estuarine sediments of the Parker River, Massachusetts. Estuar. Coasts 33, 985–1003. https://doi.org/10.1007/s12237-010-9282-5.

Weston, N.B., Vile, M.A., Neubauer, S.C., Velinsky, D.J., 2011. Accelerated microbial organic matter mineralization following salt-water intrusion into tidal freshwater marsh soils. Biogeochemistry 102, 135–151. https://doi.org/10.1007/s10533-010-9427-4.

Weston, N.B., Neubauer, S.C., Velinsky, D.J., Vile, M.A., 2014. Net ecosystem carbon exchange and the greenhouse gas balance of tidal marshes along an estuarine salinity gradient. Biogeochemistry 120, 163–189. https://doi.org/10.1007/s10533-014-9989-7.

Wieski, K., Guo, H., Craft, C.B., Pennings, S.C., 2010. Ecosystem functions of tidal fresh, brackish, and salt marshes on the Georgia coast. Estuar. Coasts 33, 161–169. https://doi.org/10.1007/s12237-009-9230-4.

Williams, A.A., Lauer, N.T., Hackney, C.T., 2014. Soil phosphorus dynamics and saltwater intrusion in a Florida estuary. Wetlands 34, 535–544. https://doi.org/10.1007/s13157-014-0520-7.

Wilson, B.J., Servais, S., Mazzei, V., Kominoski, J.S., Hu, M., Davis, S.E., Gaiser, E., Sklar, F., Bauman, L., Kelly, S., Madden, C., Richards, J., Rudnick, D., Stachelek, J., Troxler, T.G., 2018. Salinity pulses interact with seasonal dry-down to increase ecosystem carbon loss in marshes of the Florida Everglades. Ecol. Appl. 28, 2092–2108. https://doi.org/10.1002/eap.1798.

Winfrey, M.R., Zeikus, J.G., 1977. Effect of sulfate on carbon and electron flow during microbial methanogenesis in freshwater sediments. Appl. Environ. Microbiol. 33, 275–281. https://doi.org/10.1128/aem.33.2.275-281.1977.

Wood, S.A., Tirfessa, D., Baudron, F., 2018. Soil organic matter underlies crop nutritional quality and productivity in smallholder agriculture. Agric. Ecosyst. Environ. 266, 100–108. https://doi.org/10.1016/j.agee.2018.07.025.

Yang, S.C., Shih, S.S., Hwang, G.W., Adams, J.B., Lee, H.Y., Chen, C.P., 2013. The salinity gradient influences on the inundation tolerance thresholds of mangrove forests. Ecol. Eng. 51, 59–65. https://doi.org/10.1016/j.ecoleng.2012.12.049.

Zhang, J., Ross, M., 2015. Hydrologic modeling impacts of post-mining land use changes on streamflow of Peace River, Florida. Chin. Geogr. Sci. 25, 728–738. https://doi.org/10.1007/s11769-015-0745-2.

Zhang, W., Wang, C., Xue, R., Wang, L., 2019. Effects of salinity on the soil microbial community and soil fertility. J. Integr. Agric. 18, 1360–1368. https://doi.org/10.1016/S2095-3119(18)62077-5.